Effect of gas channel height on gas flow and gas diffusion in a molten carbonate fuel cell stack

Haruhiko Hirata *, Takao Nakagaki, Michio Hori

Power and Industrial Systems Research and Development Center, Toshiba, 4-1, Ukishima-cho, Kawasaki-ku, Kawasaki 210-0862, Japan

Abstract

An investigation is made of the relationships between the gas channel height, the gas-flow characteristics, and the gas-diffusion characteristics in a plate heat-exchanger type molten carbonate fuel cell stack. Effects of the gas channel height on the uniformity and pressure loss of the gas flow are evaluated by numerical analysis using a computational fluid dynamics code. The effects of the gas channel height on the distribution of the reactive gas concentration in the direction perpendicular to the channel flow are evaluated by an analytical solution of the two-dimensional concentration transport equation. Considering the results for uniformity and pressure loss of the gas flow, and for distribution of the reactive gas concentration, the appropriate gas channel height in the molten carbonate fuel cell stack is investigated. © 1999 Elsevier Science S.A. All rights reserved.

1. Introduction

In a molten carbonate fuel cell (MCFC) stack, in order to obtain a good cell performance, appropriate designs for the reactive gas transfer are necessary. The performance of the cell is affected by the gas-flow characteristics in the cell's planar and stacking direction, which in turn depends on the height of the gas channel. The influence of the gas-flow characteristics in the cell planar and stacking direction, whereby the cell performance drops because of the loss of gas-flow uniformity in each direction, have been previously investigated [1].

In order to make a height of stack compact, it is preferable for the height of the gas channel to be small. When this height is small, however, pressure losses of the flow in the gas channel increase. This requires an increase in power of the compressor or blower for driving gases and thus the efficiency of the plant will be reduced.

For flow in the cell planar direction, the height of the gas channel determines the level of influence by the viscosity and the inertia of the gases, and so it is expected that the uniformity of a cell planar direction gas-flow drops when the gas channel height is large. Furthermore,

the gas channel height affects the diffusion of the reactive gas that is supplied to the cell's active portion. For example, when the channel height is large, the diffusion time of the reactive gases increases, the reactive gas concentration on the electrode surface drops and, consequently, the diffusion overpotential will increase.

As mentioned above, the height of the gas channel is an important element for controlling the cell performance and plant efficiency in a MCFC stack. In order to determine the appropriate height of the gas channel, it is necessary to consider influences of the uniformity of the gas flow, the pressure loss, and the gas-diffusion characteristics.

In this study, the effects of a change in the gas channel height on the pressure loss and gas-flow uniformity in the cell planar direction are evaluated by computational fluid dynamics (CFD) analysis. The influences of gas channel height on the gas diffusion is evaluated by an analytical solution of the concentration transport equation, and an appropriate gas channel height for a MCFC stack is deduced.

2. Stack configuration

The configuration of a plate heat exchanger type MCFC stack is shown in Fig. 1. The electricity is generated in the

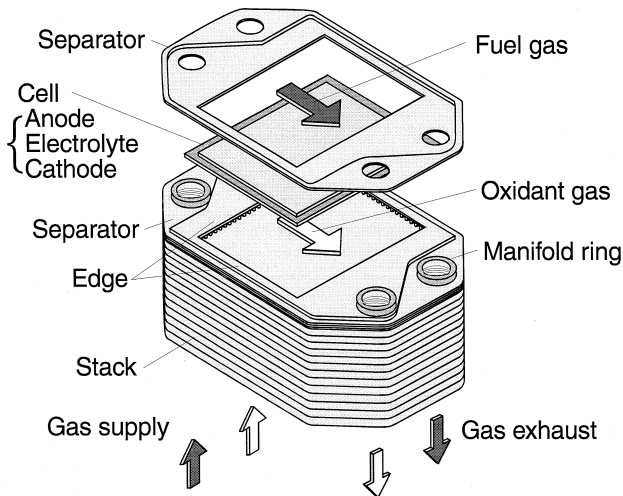* Corresponding author. Tel.: +81-44-288-8078; Fax: +81-44-288-8212; E-mail: haruhiko.hirata@toshiba.co.jp

Fig. 1. Plate heat-exchanger type stack.

Fig. 2. Three-dimension computational grid of the gas channel for CFD flow analysis.

active portion which consists of the electrolyte, the anode, and the cathode. The electrolyte consists of molten carbonate which is contained in a porous matrix. The fuel and oxidant gases are supplied via manifolds are distributed to every cell via the separator gas channels, and are finally exhausted via the exhaust manifolds.

The pressure loss in the stack is comprised of the pressure loss in the manifold and separator gas channels. The height of the gas channel has a major influence on the pressure loss in the separator gas channel. The uniformity of gas flow at the active portion is also controlled by the height of the gas channel, as well as by the shape of the inlet and the outlet portions.

The fuel and oxidant gases, flow along the electrode surfaces, and the gas composition is changed by the electrode reaction. As a consequence, the concentration distribution of the reactive gases in the gas channel height direction changes and influences the cell performance as the diffusion overpotential. Thus, concentration distribution will be mainly influenced by the gas channel height and gas utilization.

3. Method of analysis

3.1. Flow analysis

In order to investigate the effect of a change in the gas channel height on the gas-flow uniformity and pressure loss, a three-dimensional flow analysis in a plate heat exchanger type stack was conducted. CFD code PHOEN-ICS was used for the calculation. The computational grid is shown in Fig. 2. The active portion dimension is 0.9 m × 0.9 m, and the distance between the inlet-port and outlet-port is 1.35 m. The analysis was conducted for gas channel heights of 0.0014, 0.002, 0.003, and 0.005 m. The principal analysis conditions are shown in Table 1. No-slip
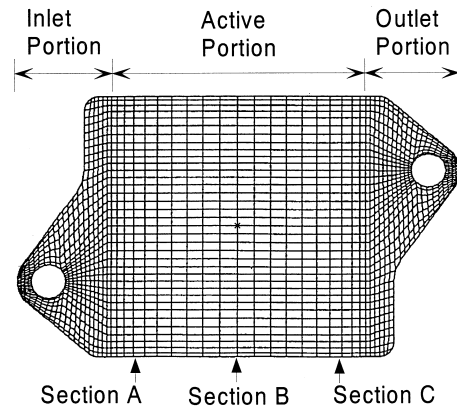
conditions on the walls of inlet and outlet portions were adopted, and in the gas channel of the active portion a friction loss coefficient (shown in Table 1) was adopted as a pressure loss caused by the current-collector in the gas channel. For the numerical mesh, BFC (Body Fitted Coordinates) were adopted in order to correspond to a curved shape; the computational domain was divided into 60 cells for the main flow direction, into 36 cells for the width direction, and 7 cells for the channel height direction.

Neglecting a chemical reaction and temperature change at the active portion and assuming that the gas conditions in the gas channel are those at the inlet-port, incompressible, steady-state, flow calculations were conducted. The flow deviations, which are mentioned later, were evaluated on Section A of the active portion inlet, on Section B of the central of active portion, and on Section C of the active portion outlet.

3.2. Analytical solution of concentration transport equation

In order to investigate the effects of the gas channel height and gas utilization on the reactive gas diffusion in the gas channel height direction, analytical solutions of the concentration transport equation were conducted.

Table 1
Principal flow analysis conditions

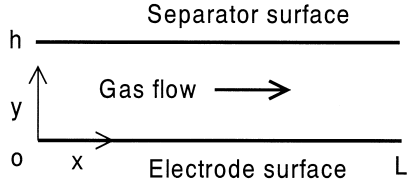|	
Inlet gas composition	Fuel $H_2:CO_2:H_2O = 70:18:12$
	Oxidant $O_2:CO_2:N_2 = 14:30:56$
Current density	1500 A/m^2
Gas utilization	Fuel 80%
	Oxidant 10%
Inlet gas temperature	923 K
Pressure	0.1 MPa
Friction loss coefficient for active portion	Fuel $\lambda_a = 106 \times Re_a^{-0.907}$
	Oxidant $\lambda_a = 14.5 \times Re_a^{-0.534}$
Reynolds number for active portion	$Re_a = 2hv_{AVE}/\nu$

Fig. 3. Two-dimensional model of gas channel in active portion for concentration transport analysis.

A summary of the two-dimension model of the active portion gas channel is shown in Fig. 3. Assuming that the movement of gas in the x direction is due only to convection and the movement of gas in the y direction is due only to diffusion, a transport equation for the molar concentration $c(x, y)$ of the reactive gases (i.e., hydrogen in the fuel or oxygen in the oxidant) in the aforementioned model can be expressed as follows [2]:

$$u\frac{\partial c}{\partial x} - D\frac{\partial^2 c}{\partial y^2} = 0 \qquad (1)$$

where: u is velocity of the flow (considered constant in the x and y directions) and D is the diffusion coefficient of the reactive gas. $D = 4.79 \times 10^{-4}$ m^2 s^{-1} for the fuel and $D = 1.23 \times 10^{-4}$ m^2 s^{-1} for the oxidant at operation temperature of 923 K, using binary diffusion coefficients of H_2–CO_2 for the fuel and O_2–N_2 for the oxidant, respectively.

The boundary conditions are based on the following assumptions: (i) in the x direction, the decrease of the reactive gas corresponds to the gas utilization U; (ii) in the y direction, the consumption of the reactive gas, which is proportional to the current density, depends on the electrode reaction on the electrode surface; (iii) there is no movement of the reactive gas on the separator surface. The boundary conditions can be expressed as follows:

$$\int_0^h c(0, y)\,dy/h = c_0, \quad \int_0^h c(L, y)\,dy/h = (1 - U)c_0 \qquad (2)$$

$$D\frac{\partial c}{\partial y} = \frac{i}{2F} \text{ (on anode)}, \quad D\frac{\partial c}{\partial y} = \frac{i}{4F} \text{ (on cathode)},$$

$$\frac{\partial c}{\partial y} = 0 \text{ (on separator)} \qquad (3)$$

where: i is current density; F is Faraday constant; c_0 is average concentration of reactive gases, which is averaged in height at the active portion inlet; h is gas channel height; L is gas channel length. The gas utilization U is defined as the rate of consumption of hydrogen in the fuel or oxygen in the oxidant from the active portion inlet to the outlet.

The reactive gas concentration in Eq. (1) can be separated into variables, i.e.,

$$c(x, y) = c_x(x)c_y(y) \qquad (4)$$

The following relation is assumed for the boundary condition of Eq. (3).

$$i(x)/c_x(x) = \text{const.} \qquad (5)$$

This assumes that the current–density distribution in the x direction is similar to the reactive gas concentration distribution in the x direction. Given this assumption, the concentration gradient of the reactive gas J on the electrode surface, that is shown later in Eq. (12), can be taken as a constant value in the x direction and separation of variables in Eq. (4) becomes possible.

In Fig. 4, a comparison is given between the distribution of current density calculated by a cell analysis code for a cell whose average current density is 1500 A m^{-2}, fuel utilization U_f is 80%, and oxidant utilization U_o is 10% [1], and the distribution of the concentration variable c_x obtained by analysis for hydrogen in the fuel. Here, the current density and concentration variable are normalized with the average current density and average concentration variable in the x direction, respectively. The distribution of c_x for hydrogen in the fuel has similar pattern to that of the distribution of the current–density, and therefore Eq. (5) is found to be applicable.

As a result of the separation of variables, the partial differential Eq. (1) is separated into the following two ordinary differential equations:

$$\frac{dc_x}{dx} - \frac{\lambda c_x}{u} = 0 \qquad (6)$$

$$\frac{d^2 c_y}{dy^2} - \frac{\lambda c_y}{D} = 0 \qquad (7)$$

Here, λ is a separation constant.

For the boundary conditions of Eq. (2), the solution for Eq. (6) is:

$$c_x = C_0 \exp(\lambda x/u) \qquad (8)$$

where $C_0 = c_0 h / \int_0^h c_y\,dy$ and is derived from a distribution of c_y which is mentioned later. Further, from the
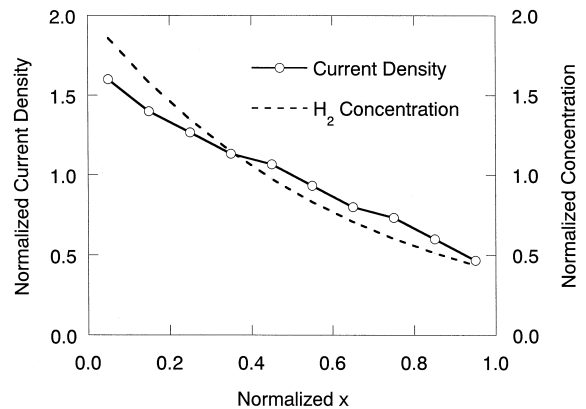

Fig. 4. Current density distribution and c_x distribution for H_2 in the fuel ($U_f = 80\%$, $U_o = 10\%$, $i_{AVE} = 1500$ Am^{-2}).

boundary conditions of Eq. (2), the separation constant λ is defined as follows.

$$\lambda = u\ln(1 - U)/L \tag{9}$$

Finally, c_x can be expressed:

$$c_x(x) = C_0\exp[x\ln(1 - U)/L] \tag{10}$$

For the boundary conditions of Eq. (3), the solution of Eq. (7) is:

$$
c_y(y)
$$
$$
= -\frac{J\left[\exp\left(y\sqrt{\frac{u\ln(1 - U)}{LD}}\right) + \exp\left((2h - y)\sqrt{\frac{u\ln(1 - U)}{LD}}\right)\right]}{\sqrt{\frac{u\ln(1 - U)}{LD}}\left[\exp\left(2h\sqrt{\frac{u\ln(1 - U)}{LD}}\right) - 1\right]} \tag{11}
$$

Here, J are the gradients of concentrations of the reactive gases on the electrode surfaces, and are derived, as follows, for the anode and cathode, respectively:

$$J = \frac{dc_y}{dy} = \frac{i}{2FDc_x}\,\text{(for anode)},$$

$$J = \frac{dc_y}{dy} = \frac{i}{4FDc_x}\,\text{(for cathode)} \tag{12}$$

In order to solve Eqs. (10) and (11), the symbolic manipulation software Maple V was used [3].

Although the result of Eq. (11) becomes a complex number, in actual calculations the imaginary part becomes less than 10^{-10} orders as a relative value to the real part, and therefore the imaginary part of Eq. (11) can be eliminated against the real part. Consequently, $c_y(y)$ is expressed as follows:

$$
c_y(y)
$$
$$
\approx \text{Re}\left\{-\frac{J\left[\exp\left(y\sqrt{\frac{u\ln(1 - U)}{LD}}\right) + \exp\left((2h - y)\sqrt{\frac{u\ln(1 - U)}{LD}}\right)\right]}{\sqrt{\frac{u\ln(1 - U)}{LD}}\left[\exp\left(2h\sqrt{\frac{u\ln(1 - U)}{LD}}\right) - 1\right]}\right\} \tag{13}
$$

Finally, c is expressed as:

$$
c(x,y) = c_x(x)c_y(y) \approx C_0\exp[x\ln(1 - U)/L]
$$
$$
\times\text{Re}\left\{-\frac{J\left[\exp\left(y\sqrt{\frac{u\ln(1 - U)}{LD}}\right) + \exp\left((2h - y)\sqrt{\frac{u\ln(1 - U)}{LD}}\right)\right]}{\sqrt{\frac{u\ln(1 - U)}{LD}}\left[\exp\left(2h\sqrt{\frac{u\ln(1 - U)}{LD}}\right) - 1\right]}\right\} \tag{14}
$$

Also, the diffusion velocity w_y of the reactive gas in the gas channel height direction is derived as:

$$
w_y(y) = -\frac{D}{c}\frac{\partial c}{\partial y} \approx \text{Re}\left\{\sqrt{\frac{Du\ln(1 - U)}{L}}\right.
$$
$$
\left.\times\frac{-\exp\left(y\sqrt{\frac{u\ln(1 - U)}{LD}}\right) + \exp\left((2h - y)\sqrt{\frac{u\ln(1 - U)}{LD}}\right)}{\exp\left(y\sqrt{\frac{u\ln(1 - U)}{LD}}\right) + \exp\left((2h - y)\sqrt{\frac{u\ln(1 - U)}{LD}}\right)}\right\} \tag{15}
$$

From the results of Eqs. (14) and (15), the concentration distribution and diffusion velocity distribution of the reactive gas are found to be affected by the gas channel height h and gas utilization U.

The concentration distribution c_y in y direction and the diffusion velocity distribution w_y in y direction were calculated using Eqs. (13) and (15), respectively. Here, the gas channel length L is 0.9 m, and for i and c_x in Eq. (12), an average current density of 1500 A m^{-2} is assumed for i and c_0 is used for c_x as a representative value in the x direction. The value of c_0 is taken as 0.70 for hydrogen in the fuel and 0.14 for oxygen in the oxidant. The active portion inlet velocity which is determined by the gas utilization and average current density, was used as u for both the fuel and the oxidant.

4. Results and discussion

4.1. Effect of gas channel height on pressure loss

From the flow analysis results, the relations between the gas channel height and the pressure loss have been investigated.

The pressure contours derived from the three-dimensional flow analysis for gas channel heights of 0.0014 m and 0.005 m for the fuel flow and the oxidant flow are shown in Figs. 5 and 6, respectively. The pressure distribution patterns do not change significantly with the variation of the gas channel height. In each case, the pressure drop in the inlet and outlet portions is larger than that in the active portion, and the pressure drop in each portion decreases with increasing gas channel height.

The pressure loss coefficient between the inlet-port and outlet-port for each gas channel height for the fuel flow and oxidant flow, is shown in Fig. 7. The pressure loss coefficient ζ is defined as follows when the flow velocities at the inlet and outlet are taken to be the same:

$$\zeta \equiv \frac{P_{\text{in}} - P_{\text{out}}}{\rho v_{\text{AVE}}^2/2} \tag{16}$$

where: P_{in} is static pressure at the inlet, P_{out} is the static pressure at the outlet; ρ is the density; v_{AVE} is the average flow velocity in the active portion.
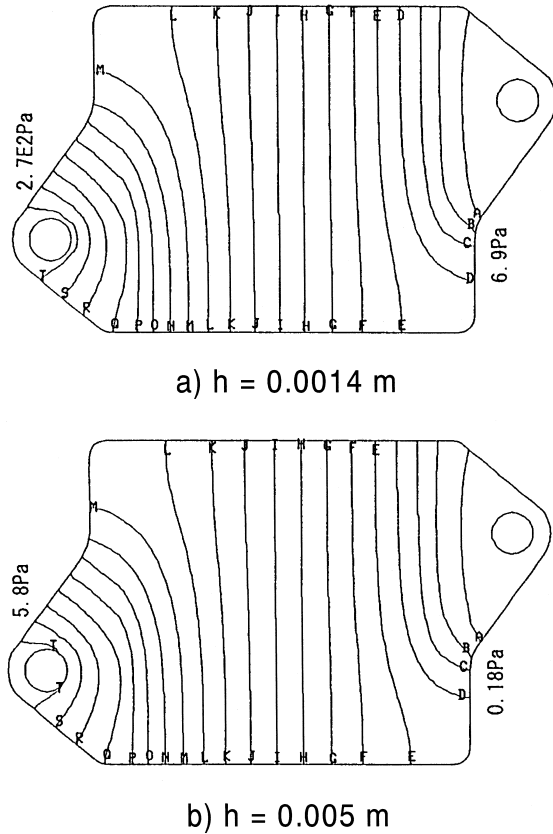
a) h = 0.0014 m

b) h = 0.005 m

Fig. 5. Pressure contours of fuel flow for various gas channel heights, h.

The pressure loss coefficient decreases and the pressure loss drops with increase in the gas channel height for the fuel and oxidant. Compared with the case for a gas channel height of 0.0014 m, the pressure loss coefficient for a gas channel height of 0.003 m drops 54% for the fuel and 51% for the oxidant with increasing gas channel height. The decrease of the pressure loss coefficient becomes smaller until it is found to be almost saturated when the gas channel height is 0.005 m. Consequently, increasing the gas channel height from 0.003 m to 0.005 m results in a smaller reduction in the pressure loss coefficient, i.e., 29% for the fuel and 36% for the oxidant.

Generally, in order to make a stack more compact, it is preferable for the height of the gas channel to be made small. From the above results, however, in order to lower the pressure loss through a stack, the gas channel height should be large. Further, the reduction of the pressure loss by increasing the gas channel height is almost saturated when the gas channel height is 0.005 m. The effect of an increase in the gas channel height on the pressure loss is thought to be small when the height is more than 0.005 m.

4.2. Effect of gas channel height on gas-flow uniformity

From the flow analysis results, the relations between the gas channel height and the uniformity of gas flow have been investigated.

The flow deviation of the fuel and oxidant flow on Sections A, B, and C for various gas channel heights is shown in Fig. 8. Here, the flow deviation σ is a parameter used to evaluate the uniformity of flow in each section, and is defined with the standard deviation and the root mean square of the flow velocity component v_i which is in a direction perpendicular to the section as follows:

$$\sigma = \frac{\sqrt{\left\{ \sum_{i=1}^{n} \left(v_i - v_{\mathrm{AVE}} \right)^2 \right\}/n}}{\sqrt{\left(\sum_{i=1}^{n} v_i^2 \right)/n}}, \qquad v_{\mathrm{AVE}} = \frac{\sum_{i=1}^{n} v_i}{n} \qquad (17)$$

Consequently, the uniformity of flow on the section becomes good when the flow deviation is low.

With respect to both the fuel flow and oxidant flow, the flow deviation on Section B of the active portion center is one-tenth smaller than that on Section A of the active portion inlet and Section C of the active portion outlet for each gas channel height.

For the fuel, flow deviation changes caused by an increase in the gas channel height from 0.0014 to 0.005 m are 34.3 to 34.5% on Section A, 0.791 to 0.742% on Section B, and 24.3 to 25.3% on Section C. For the oxidant, flow deviation changes caused by an increase in
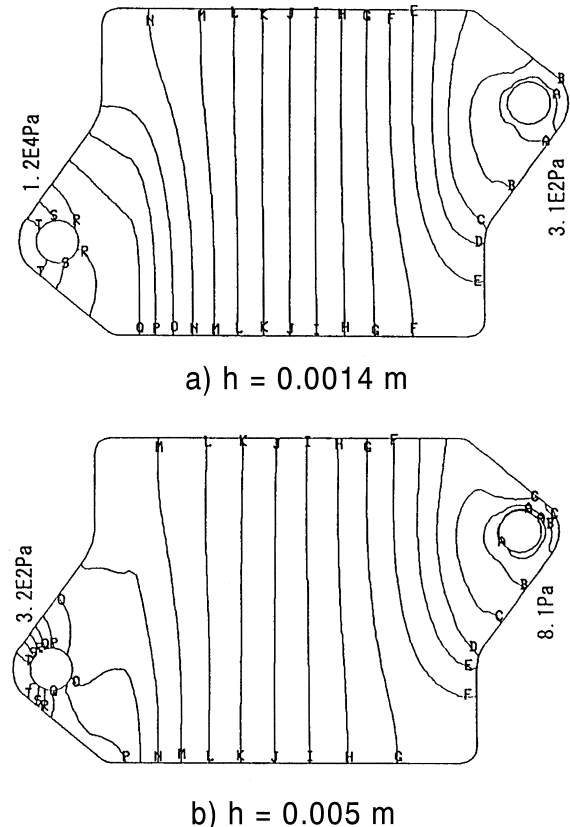

a) h = 0.0014 m

b) h = 0.005 m

Fig. 6. Pressure contours of oxidant flow for various gas channel heights, h.
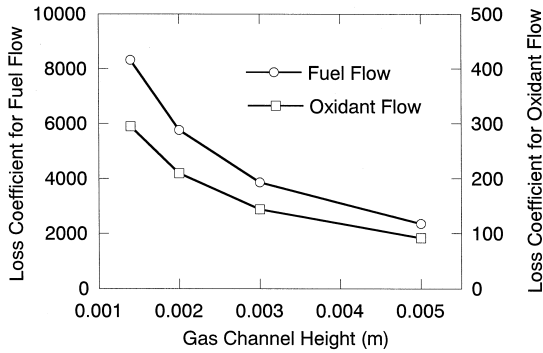
Fig. 7. Effect of gas channel height on pressure loss.

a) H_2 concentration distribution

b) H_2 diffusion velocity distribution

Fig. 9. H_2 concentration and diffusion velocity distribution in fuel in y direction for various gas channel heights ($U_f = 80\%$).

the gas channel height from 0.0014 to 0.005 m are 26.6 to 26.7% on Section A, 0.197 to 1.53% on Section B, and 21.5 to 25.6% on Section C. Thus, except in the case of Section B for the oxidant, the flow deviation changes caused by the gas channel height change are small.

In cases where the flow deviations on the active portion inlet are less than 50%, it has been found that the effect of the flow uniformity on the cell voltage is less than 1% [1]. Consequently, in the separator gas channel, although the increase of the gas channel height results in some increase in the flow deviation, the effect on the cell performance is found to be small, for both the fuel flow and the oxidant flow.
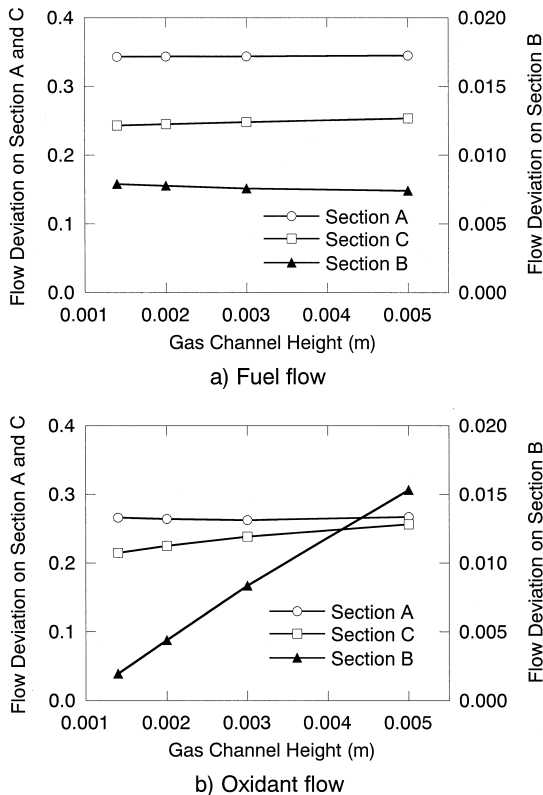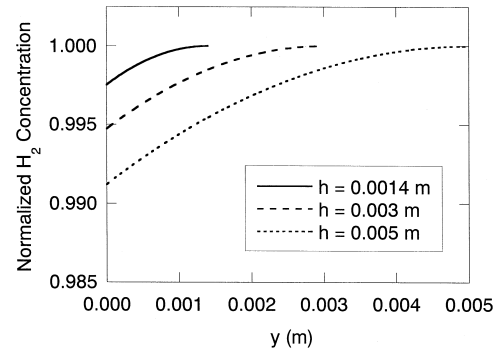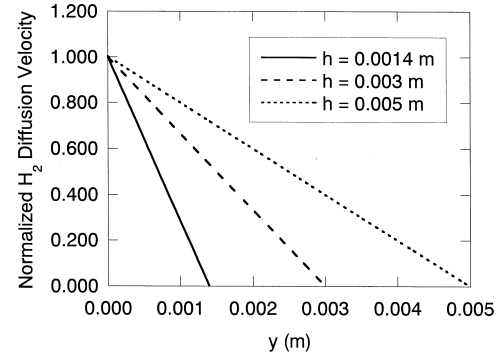
4.3. Effect of gas channel height on gas diffusion

From the results of the analytical solution of the concentration transport equation, the relations between the gas channel height, gas utilization, and the reactive gas diffusion in the gas channel height direction have been investigated.

Fig. 9 shows the concentration and diffusion velocity distribution of hydrogen in the fuel for a utilization U_f of 80%, and a gas channel height, h, of 0.0014, 0.003 m or 0.005 m. Here, the concentration distribution is normalized so that the concentration on the separator surface is unity in each height case, and the diffusion velocity is normalized so that the diffusion velocity on the electrode surface is unity in the case for $h = 0.003$ m.

For all gas channel heights, the hydrogen concentration is reduced on proceeding from the separator surface to the electrode surface. The hydrogen concentration on the electrode surface becomes lower, that is, 0.998, 0.995, and 0.991, in accordance with increase in the gas channel height, that is, 0.0014, 0.003 and 0.005 m, respectively. The concentration drop on the electrode surface is merely 0.9% for a gas channel height of 0.005 m, and this is the largest drop.

The concentration and diffusion velocity distribution of oxygen in the oxidant for a utilization U_o of 10%, and a gas channel height, h, of 0.0014, 0.003 or 0.005 m are
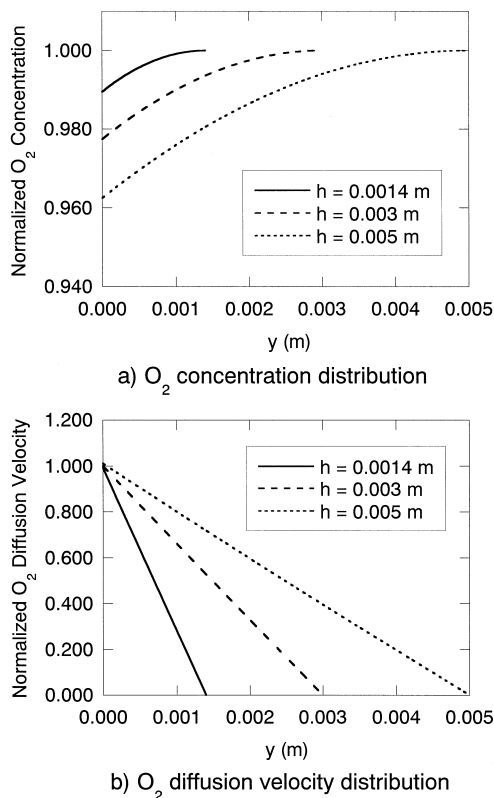

a) Fuel flow

b) Oxidant flow

Fig. 8. Effect of gas channel height on flow deviation.

a) O$_2$ concentration distribution

b) O$_2$ diffusion velocity distribution

Fig. 10. O$_2$ concentration and diffusion velocity distribution in oxidant in y direction for various gas channel heights ($U_o = 10\%$).

shown in Fig. 10. For all gas channel heights, the oxygen concentration is reduced on proceeding from separator surface to the electrode surface. The oxygen concentration on the electrode surface becomes lower, that is, 0.989, 0.977 and 0.962, as the gas channel height is increased, that is, 0.0014, 0.003, and 0.005 m, respectively. The concentration drop on the electrode surface is merely 3.8% when the gas channel height is 0.005 m, and this is the largest drop. The drop in oxygen concentration on the electrode surface is larger compared with that for the fuel, and this is thought to be due to the fact that the diffusion coefficient of oxygen in the oxidant is smaller than that of hydrogen in the fuel.

For the diffusion velocities of hydrogen and oxygen shown in Figs. 9 and 10, the distribution patterns are almost linear, and therefore the concentration distributions of hydrogen and oxygen are found to be almost quadratic, although they are expressed as the complicated function shown in Eq. (14). Furthermore, the diffusion velocities on the electrode surface vary little with change in the gas channel height for the fuel and oxidant.

The distribution of the concentration and diffusion velocity of hydrogen in the fuel for a gas channel height of 0.003 m and a utilization U_f of 50, 80, and 95% is shown in Fig. 11. Here, the concentration distribution is normalized so that the concentration on the separator surface is unity in each utilization case, and the diffusion velocity is

normalized so that the diffusion velocity on the electrode surface is unity in the case for $U_f = 80\%$.

For all utilizations, the hydrogen concentration falls on proceeding from the separator surface to the electrode surface. The hydrogen concentration on the electrode surface becomes lower, that is, 0.996, 0.995, and 0.992, in accordance with an increase in the utilization of 50, 80, and 95%, respectively. The concentration drop on the electrode surface is merely 0.8% when the utilization is 95%, and this is the largest drop.

The diffusion velocities on the electrode surface become larger, that is, 0.688, 1.00, and 1.58, with as the utilization increases by 50, 80, and 95%, respectively. The increase rate of the diffusion velocity also becomes larger when the utilization becomes high.

The distribution of the concentration and diffusion velocity of oxygen in the oxidant for a gas channel height of 0.003 m and a utilization U_o of 10, 20, and 40% is shown in Fig. 12. Here, the diffusion velocities are normalized so that the diffusion velocity on the electrode surface is unity in the case for $U_o = 10\%$.

For all utilizations, the oxygen concentration is reduced as proceeding from the separator surface to the electrode surface. The oxygen concentration on the electrode surface becomes lower, that is, 0.977, 0.976, and 0.973, with increase in the utilization, that is, 10, 20, and 40%, respectively. The concentration drop on the electrode surface is
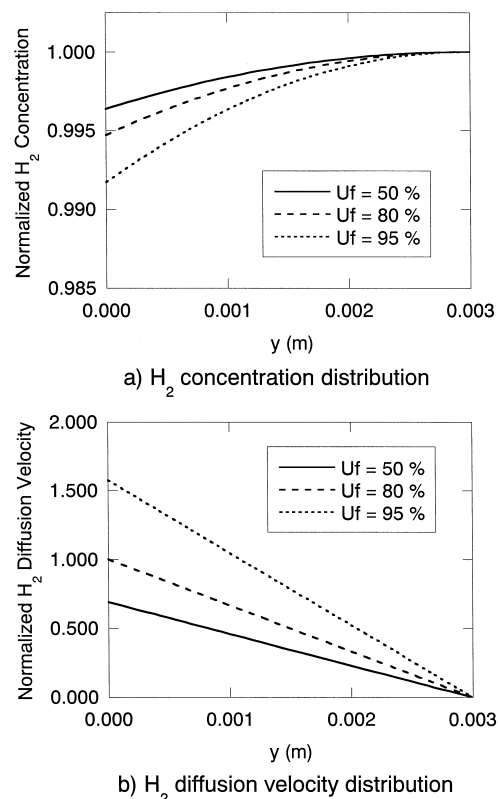

a) H$_2$ concentration distribution

b) H$_2$ diffusion velocity distribution

Fig. 11. H$_2$ concentration and diffusion velocity distributions in the fuel in the y direction for various fuel utilizations ($h = 0.003$ m).

merely 2.7% when the utilization is 40%, and this is the largest drop.

The diffusion velocity on the electrode surface become larger, that is, 1.00, 1.06, and 1.22, as the utilization increases, i.e., 10, 20, and 40%, respectively. The increase rate of the diffusion velocity also becomes larger when the utilization becomes high.

The change in the reactive gas concentration on the electrode surface caused by changes in the gas channel height and utilization, for hydrogen in the fuel and oxygen in the oxidant, are presented in Fig. 13. Here, the reactive gas concentration is normalized so that the concentration on the separator surface is unity in each case.

The concentration of hydrogen on the electrode surface drops linearly with increase in the gas channel height, for each utilization. As the utilization increases, the concentration of hydrogen on the electrode surface drops, and the rate of decline increases as the gas channel height increases. Consequently, the drop of hydrogen concentration on the electrode surface is merely 1.4% when the utilization is 95% and the gas channel height is 0.005 m, and this is the largest drop. Therefore, the effect of the hydrogen diffusion in the fuel on the electrode reaction as a diffusion overpotential is found to be small.

The concentration of oxygen on the electrode surface falls linearly with increase in the gas channel height, for each utilization. As the utilization increases, the concentra-
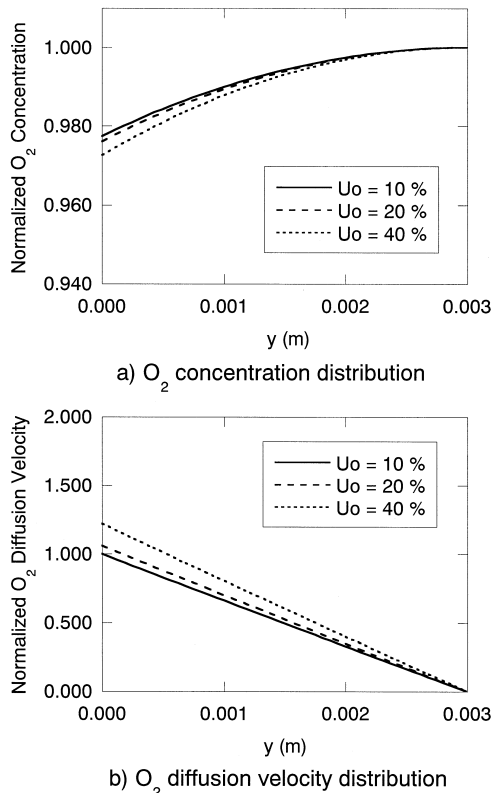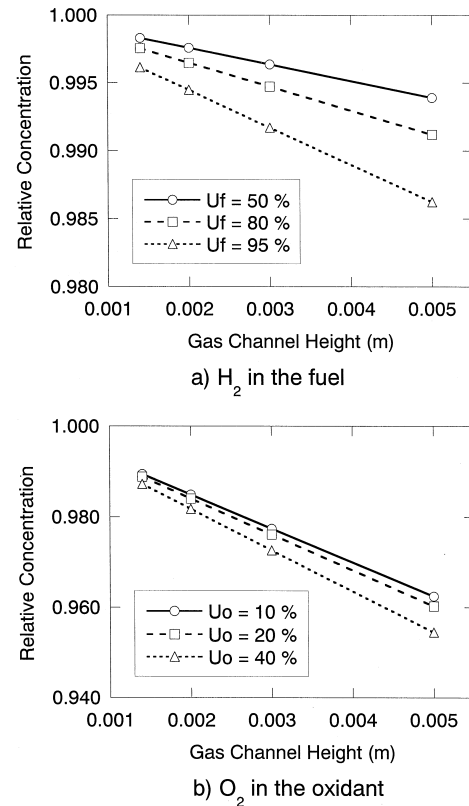

a) H_2 in the fuel

b) O_2 in the oxidant

Fig. 13. H_2 and O_2 concentration on electrode surface relative to concentration on separator surface.

tion of oxygen on the electrode surface falls at a rate which increases as the gas channel height increases. Consequently, the drop in oxygen concentration on the electrode surface is merely 4.6%, when the utilization is 40% and the gas channel height is 0.005 m, and this is the largest drop. Therefore, the effect of the oxygen diffusion in the oxidant on the electrode reaction as a diffusion overpotential is found to be smaller than in the case of the fuel. This is because the utilization of the oxidant is lower than that of the fuel.

5. Conclusions

In a plate heat-exchanger type molten carbonate fuel cell stack, the effect of a change in the gas channel height on the pressure loss, the uniformity of the gas flow, and the gas diffusion has been evaluated by numerical flow analysis and analytical solution of the concentration transport equation. The following results have been obtained.

(i) With an increase in the gas channel height, the pressure loss drops and this drop is almost saturated at a gas channel height of 0.005 m.

(ii) With an increase in the gas channel height, the uniformity of the gas flow drops; the flow deviation is 35% when the gas channel height is 0.005 m, and the influence on the cell performance is small.

a) O_2 concentration distribution

b) O_2 diffusion velocity distribution

Fig. 12. O_2 concentration and diffusion velocity distribution in oxidant in y direction for various oxidant utilizations ($h = 0.003$ m).

(iii) With an increase in the gas channel height, the reactive gas concentration on the electrode surface drops, but the drop in the reactive gas concentrations is merely 1.4% for the fuel and 4.6% for the oxidant when the gas channel height is 0.005 m. This is the largest reduction, and therefore the effect of an increase in the gas channel height on the diffusion overpotential is small.

(iv) When the height of separator gas channel is below 0.005 m, the decline in cell performance, which depends on the influence of the uniformity of the gas flow and the gas diffusion, is small appropriate gas channel height can be determined based on the relation with the pressure loss and the size of the MCFC stack.

6. List of symbols

c	Molar concentration $(\mathrm{mol/m^3})$
c_x	Molar concentration x variable $(-)$
c_y	Molar concentration y variable $(\mathrm{mol/m^3})$
c_0	Molar concentration at inlet $(\mathrm{mol/m^3})$
D	Diffusion coefficient $(\mathrm{m^2/s})$
F	Faraday constant 96487 $(\mathrm{A \cdot s/mol})$
h	Gas channel height (m)
i	Current density $(\mathrm{A/m^2})$
J	Molar concentration gradient $(\mathrm{mol/m^4})$
L	Gas channel length (m)
P	Static pressure (Pa)
Re_a	Reynolds number for active portion $(-)$
u	Flow velocity (m/s)
U	Gas utilization $(-)$
v	Flow velocity (m/s)
v_{AVE}	Average flow velocity for active portion (m/s)
w_y	Diffusion velocity (m/s)

Greek letters

ν	Kinetic viscosity for gas $(\mathrm{m^2/s})$
λ	Separation constant $(\mathrm{s^{-1}})$
λ_a	Friction loss coefficient for active portion $(-)$
ρ	Gas density $(\mathrm{kg/m^3})$
σ	Flow deviation $(-)$
ζ	Pressure loss coefficient $(-)$

Operator symbols

Re	Real part

Subscripts

f	Fuel
o	Oxidant
in	Inlet
out	Outlet

Acknowledgements

References

[1] H. Hirata, M. Hori, Journal of Power Sources 63 (1996) 115–120.
[2] W.N. Gill, R. Sankarasubramanian, Proc. R. Soc. London, A 316 (1970) 341–350.
[3] K.M. Heal, M.L. Hansen, K.M. Rickard, Maple V Learning Guide, Springer, New York, 1996, p. 77.